Electronic Supplementary Information (ESI)

In situ synthesis of needle-shaped bimetallic organic frameworks on highly porous graphene scaffolds for efficient electrocatalytic water oxidation

Behnam Nourmohammadi Khiarak [1], Mahdi Hasanzadeh [2], Majdoddin Mojaddami [1], Hossein Shahriyari Far [3], Abdolreza Simchi [1,4*]

[1] Department of Materials Science and Engineering, Sharif University of Technology, Azadi Avenue, P.O. Box 11365-8639, Tehran, Iran

[2] Department of Textile Engineering, Yazd University, P.O. Box 89195-741, Yazd, Iran

[3] Department of Chemistry, Iran University of Science and Technology, Narmak, P.O. Box 16846-13114, Tehran, Iran

[4] Institute for Nanoscience and Nanotechnology, Sharif University of Technology, Azadi Avenue, P.O. Box 11365-8639, Tehran, Iran

b.nourmohammadi1994@gmail.com *(B. N. Khiarak)*

M.hasanzadeh@yazd.ac.ir *(M. Hasanzadeh)*

m.mojaddami@chmail.ir *(M. Mojaddami)*

h_shahriyarifar@alumni.iust.ac.ir *(H. Shahriyari Far)*

** Corresponding author. E-mail: simchi@sharif.edu; Fax: +98 21 66005717; Tel: +98 21 6616 5261*

S1. Experimental section

Materials

Cobalt (II) chloride hexahydrate ($CoCl_2.6H_2O$), nickel (II) chloride hexahydrate ($NiCl_2.6H_2O$), terephthalic acid (TPA, 98%), *N*,*N*-dimethylformamide (DMF, 99.8%), and ethanol were bought from Merck Co. (Germany) and used directly without further purification. Ni foam (NF, 99.9 % purity) was provided from Nano Bazar (Tehran, Iran).

Synthesis of 3D graphene structure

3D graphene was prepared by chemical vapor deposition (CVD) according to the procedure reported elsewhere [1]–[3]. The Ni foam was cut into small parts with dimensions of 0.012 × 1 × 4 cm^3 and ultrasonically cleaned in 3 M HCl, acetone, ethanol, and DI water for 10 min. The cleaned specimens were dried under nitrogen gas flow and placed into a quartz boat in a tube furnace. The sample was heated from ambient temperature to 1050°C with a rate of 15 $°C.min^{-1}$ under the flow of Ar (450 sccm)/H_2 (50 sccm) gas mixture. A dwell time of 15 min was considered at the temperature to anneal the Ni substrate and to remove oxide layers. Thereafter, the reaction was allowed to proceed for about 20 min under the flow of CH_4 (20 sccm) and the Ar/H_2 mixture. In following, the furnace was turned off and the flow of CH_4 was stopped. The sample was then removed from the hot zone and cooled under the Ar/H_2 gas mixture.

Synthesis of MOFs/3D graphene

Highly porous (Co, Ni) MOFs/3DG electrodes with different Co/Ni ratios were synthesized by in situ solvothermal deposition of MOFs [4] on 3DG/NF. A mixture of DMF (32 ml), ethanol (2 ml), DI water (2 ml), and terephthalic acid (0.125 g, 0.75 mmol) was prepared and homogenized by sonication. $CoCl_2.6H_2O$ and $NiCl_2.6H_2O$ at specified ratios were then added

to the mixture. The ratio of Co and Ni precursors was selected to attain MOFs with different Co_x/Ni_{1-x} compositions ($0 \leq x \leq 1$). The solutions were transferred into a Teflon-lined autoclave containing 3DG/NF scaffolds. The processing temperature and time were 140°C and 48 h, respectively. The electroactive electrodes were obtained by drying at 70°C for 8 h.

Materials characterizations

X-ray diffraction (Philips, X'pert PRO, Netherlands, Cu Kα, 1.545 Å) was employed for phase analysis. Raman spectroscopy (Teksan, Takram P50C0R10, Nd:YAG laser) was utilized to study the structure of 3DG. Field-emission scanning electron microscopy (SEM) equipped with energy-dispersive spectroscopy instrument (Zeiss, Germany) was used for microstructural observations and elemental analyses. Transmission electron microscopy (TEM, Philips, Netherland) was conducted to study the MOF/3DG morphology. Fourier transformed infrared (FTIR) spectra were recorded on AVATAR FTIR instrument (Thermo Nicolet, USA). MicroActive-TriStar II Plus 2.03 Instrument was employed to study the specific surface area and pore size distributions of 3DG by Brunauere-Emmmette-Teller (BET) and Barrett-Joyner-Halenda (BJH) methods.

Electrochemical measurements

All electrochemical experiments for OER reaction were conducted by an Autolab PGSTAT 302 N electrochemical workstation (Metrohm Autolab, Netherlands) at ambient condition. The as-prepared electrocatalysts were used as the working electrodes with the size of ~ 1 cm^2, a platinum rod as counter electrode, and Ag/AgCl (KCl 3 M) as the reference electrode and KOH 1M as electrolyte for OER.

S2. Specific surface area and pore size of 3DG substrate

Fig. S1 shows the BET isotherm and BJH pore size distribution of 3DG substrate. The material exhibits the type III isotherm with small hysteresis loop. This observation suggests the mesoporous feature of the 3DG structure. The BJH plot supports the mesopore structure of 3DG with a mean pore diameter of about 2.4 nm. The specific surface area is about 34 $m^2.g^{-1}$. The open pore structure of 3DG (200-500 μm) provides efficient ion diffusion pathway for rapid transfer of electrolyte ions especially at high current density.

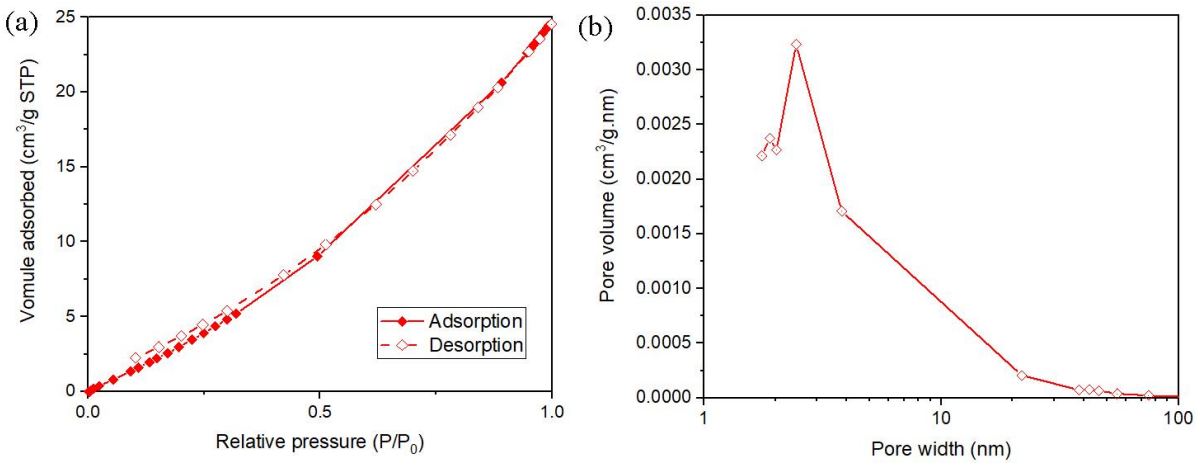

Fig. S1. (a) Nitrogen adsorption/desorption isotherm and (b) BJH pore size distribution of the 3DG structure.

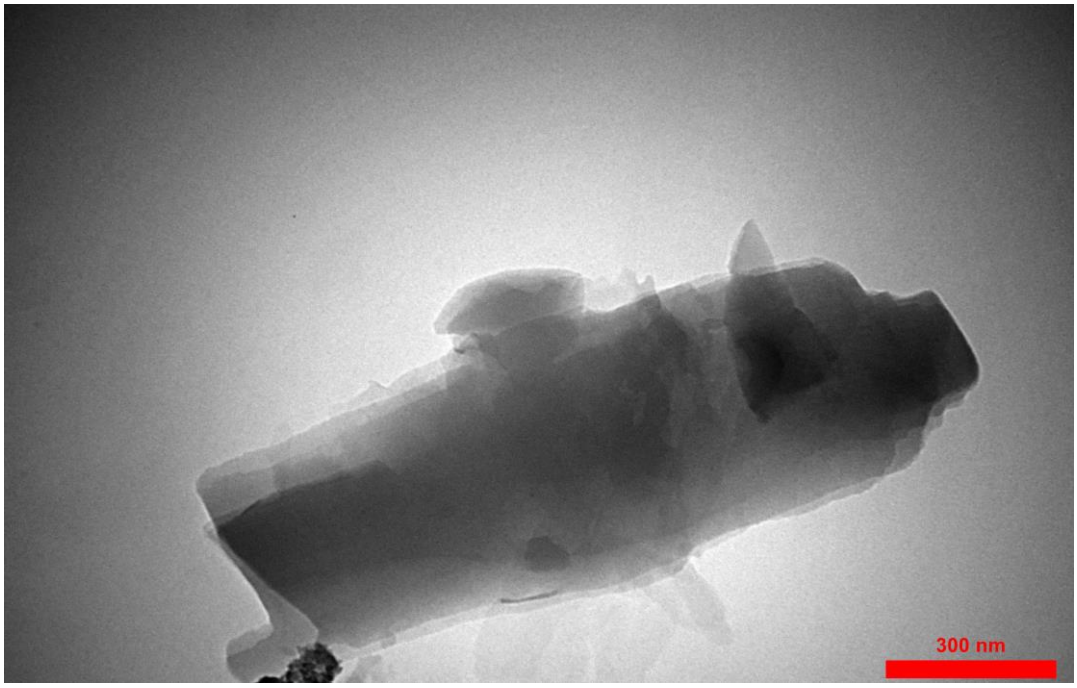

Fig. S2. TEM micrograph shows $Co_{0.3}Ni_{0.7}$ MOF plates.

S3. FTIR studies

Fig. S3 shows FTIR spectra of $Co_{0.3}Ni_{0.7}$ MOF and $Co_{0.3}Ni_{0.7}$ MOF/3DG. The peaks at 1583 and 1681 cm^{-1} are related to the asymmetric stretching of (-COO-) groups in the TPA ligand [5]. The band at 1383 cm^{-1} is also assigned to the symmetric stretching vibrations of these groups. The small peak at 1506 cm^{-1} is attributed to C=C of benzene ring [6]. The bands at 2976 and 2878 cm^{-1} are assigned to CH_2 stretching vibrations. The bands appeared at 1300–1000 cm^{-1} correspond to CO stretch in carboxylic group and C-H deformation vibration of benzene ring. The bands at 3521 and 3600 cm^{-1} are assigned to free OH bond [7]. Only a new adsorption peak at around 973 cm^{-1} was detected in the spectrum $Co_{0.3}Ni_{0.7}$ MOF/3DG that might be due to possible chemical reactions between bimetallic CoNi MOF and the 3DG substrate.

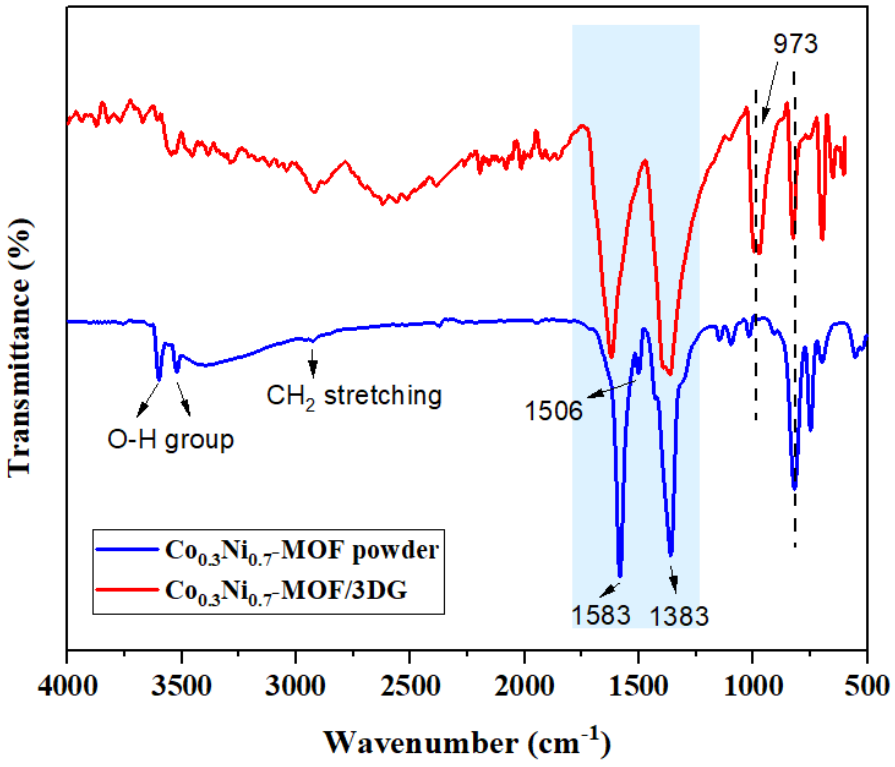

Fig. S3. FTIR spectrum of $Co_{0.3}Ni_{0.7}$ MOF and $Co_{0.3}Ni_{0.7}$ MOF/3DG.

S4. Electrochemical active surface area

Fig. S4 shows CV plots for the examined electrode at different scan rates (ν). The slope of the current density verses the scan rate is related to the capacitance (C) of electrode which is a measure of electrochemical active surface area. Ni foam has a C value of 6×10^{-6} $F.cm^{-2}$. CVD of graphene on the Ni foam significantly increased the C value by more than 33.3 times (2×10^{-4} $F.cm^{-2}$). After in situ synthesis of CoNi-based MOF on 3DG, the C value was further enhanced to 2.5×10^{-3} $F.cm^{-2}$. These results could evidence that the active surface area of the CoNi-based MOF/3DG is much higher than the 3DG and Ni foam substrates, which is important for electrochemical applications.

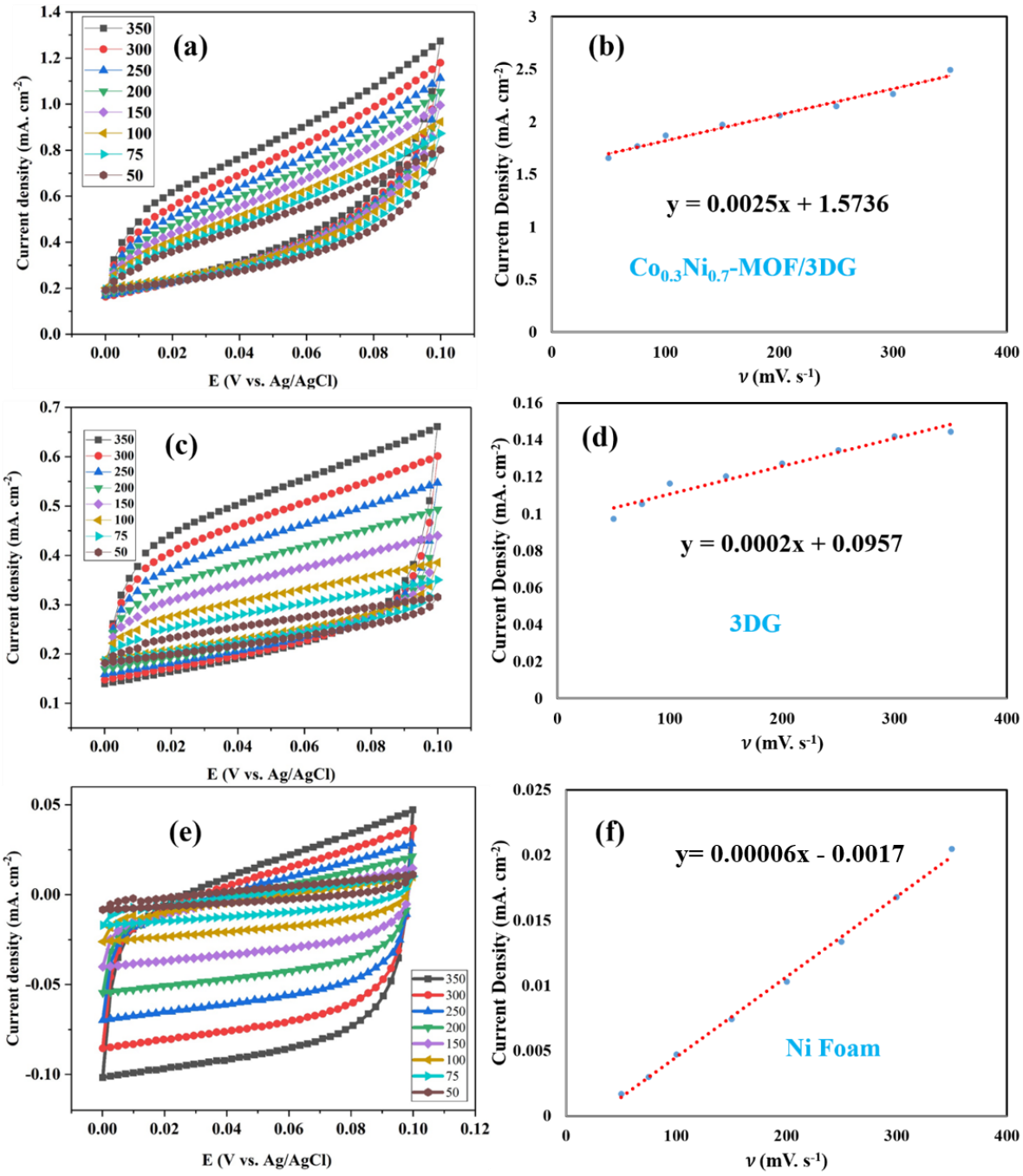

Fig. S4. Estimation of electrochemical surface area via capacitance measurements. CV plots at different scan rates in the range of 50 to 350 mV.s^{-1} for (a) $Co_{0.3}Ni_{0.7}$ MOF/3DG, (c) 3DG, and (e) Ni foam. Corresponding capacitive currents for (b) $Co_{0.3}Ni_{0.7}$ MOF/3DG, (d) 3DG, and (f) Ni foam.

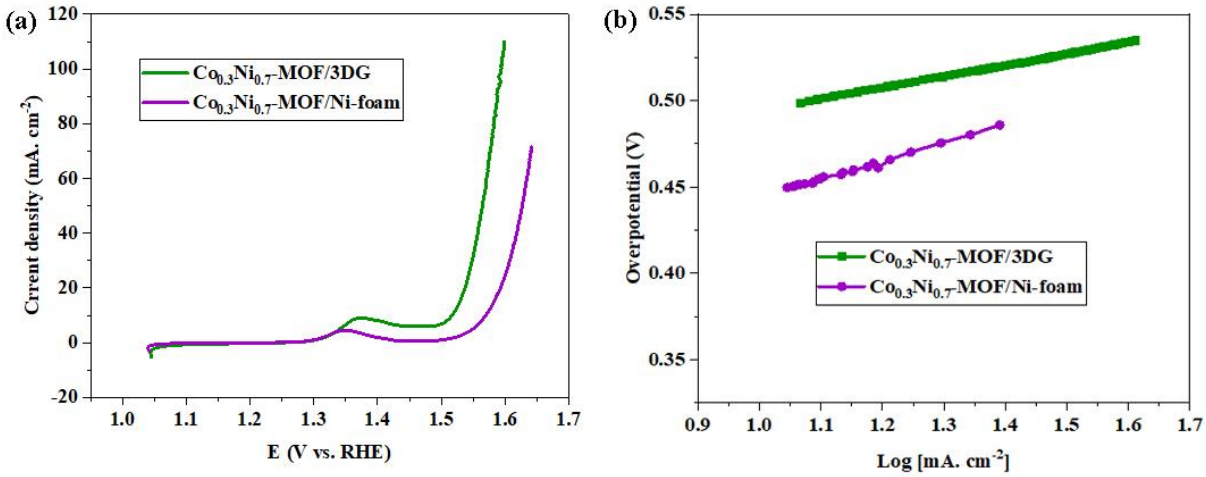

Fig. S5: (a) LSV and (b) Tafel plots for $Co_{03}Ni_{0.7}$-MOF and $Co_{03}Ni_{0.7}$-MOF/3DG.

Table S1. Tafel slope of the prepared $Co_{0.3}Ni_{0.7}$ MOF/3DG electrocatalyst as compared with other nanostructures reported in the literature

Catalyst	Electrolyte	Tafel slope mV. dec^{-1}	Reference
Ni-doped CoP-based MOF	1 M KOH	69	[8]
N-doped carbon nanotube frameworks	1 M KOH	93	[9]
Spindle-like Co/Fe metal oxides in N-doped porous carbon	0.1 M KOH	79	[10]
Co NPs* embedded in porous N-rich carbon	1 M KOH	76	[11]
MOF-derived Zn-doped $CoSe_2$	1 M KOH	88	[12]
Co/Co_9S_8@S,N-doped porous graphene sheets assembled Co-MOFs	0.1 M KOH	80.2	[13]
$Co_{0.3}Ni_{0.7}$ MOF/3DG	1 M KOH	66.4	This work

*Nanoparticles

Table S2. OER performance of $Co_{0.3}Ni_{0.7}$ MOF/3DG as compared with some representative non-precious metals electrocatalysts

Catalyst	Electrolyte	Current density ($mA.cm^{-2}$)	Overpotential at the corresponding current density (mV)	Reference
Ni_5P_4/NF	1 M KOH	10	470	[14]
NiFe-LDH/NF	1 M NaOH	10	470	[15]
$Ni(OH)_2/NiSe_2$/CC[1]	1 M KOH	10	550	[16]
$NiCo_2S_4$ nanowires/CC	1 M KOH	20	620	[17]
NiFeZn-MOF-nanosheets/NF	1 M KOH	40	350	[18]
PNG[2]-$NiCo_2O_4$	1 M KOH	20	~ 593	[19]
Ni-NP/N-Gr/Ni-based MOF/NF	1 M KOH	20	300	[20]
Co-based MOF/Co@N-C	0.1 M KOH	15	370	[21]
Co-P/NC[4]/CC	1 M KOH	20	345	[22]
NiS_2/CoS_2/CC	1 M KOH	20	310	[23]
$NiCo_2O_4@Ni_3S_2$/NF	1 M KOH	40	360	[24]
MOF-based CoP/rGO	1 M KOH	10	350	[25]
Spindle-like Co/Fe metal oxides in N-doped porous carbon	0.1 M KOH	10	390	[10]
Mo-NiCoP	1 M KOH	20	390	[26]
$Co_{0.3}Ni_{0.7}$ MOF/3DG/NF	1 M KOH	20	291	This work

[1]Carbon Cloth, [2]Porous Nitrogen-doped Graphene, [3] Covalent-Organic Frameworks and [4]Nitrogen containing carbon

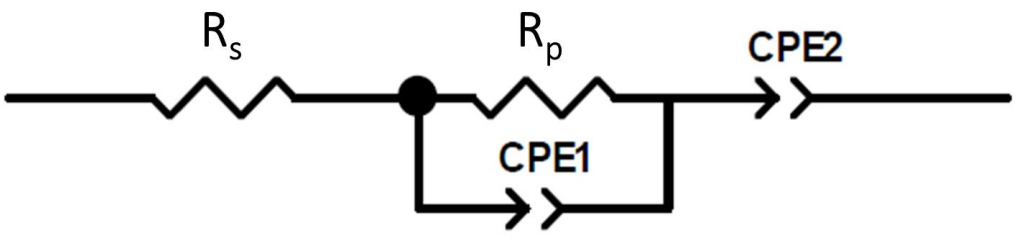

Fig. S6. Equivalent circuit used to fit the EIS data. In this equivalent circuit, R_S is series resistance due to solution, wiring and other uncompensated resistances. R_P is related to charge transfer resistance. CPE_1 is attributed to double layer capacitance on a non-uniform surface. CPE_2 is related to transport phenomena in the electrolyte [27].

Table S3. Equivalent circuit parameters obtained from fitting the EIS data based on the equivalent circuit shown in ESI Fig. S6.

MOF on 3DG/NF	R_s (Ω)	CPE_1-T ($F.cm^{-2}$)	CPE_1-P	R_P ($\Omega.cm^{-2}$)	CPE_2-T ($F.cm^{-2}$)	CPE_2-P
Reference†	2.72	0.306	0.87	7.98	0.189	0.37
Ni	3.506	0.001	0.6159	6.44	0.306	0.53
Co	4.02	0.245	0.26	5.05	0.190	0.72
$Co_{0.3}Ni_{0.7}$	2.29	0.044	0.47	1.82	0.811	0.67
$Co_{0.5}Ni_{0.5}$	3.14	0.103	0.30	3.95	0.357	0.54
$Co_{0.7}Ni_{0.3}$	3.04	0.115	0.31	10.50	0.083	0.59

† 3DGF electrode without MOF

S5. Stability test

Fig. S7 shows EDS and XRD patterns of the MOF/3DG electrode before and after the stability test. The EDS peaks of Co and Ni after the stability test were not remarkably reduced after the examination. In the XRD pattern of the electrode only the characteristic peaks of Ni at 44.38°, 51.72° and 76.16° corresponding to (111), (020) and (222) planes, respectively, were visible because the amount of Ni was dominant.

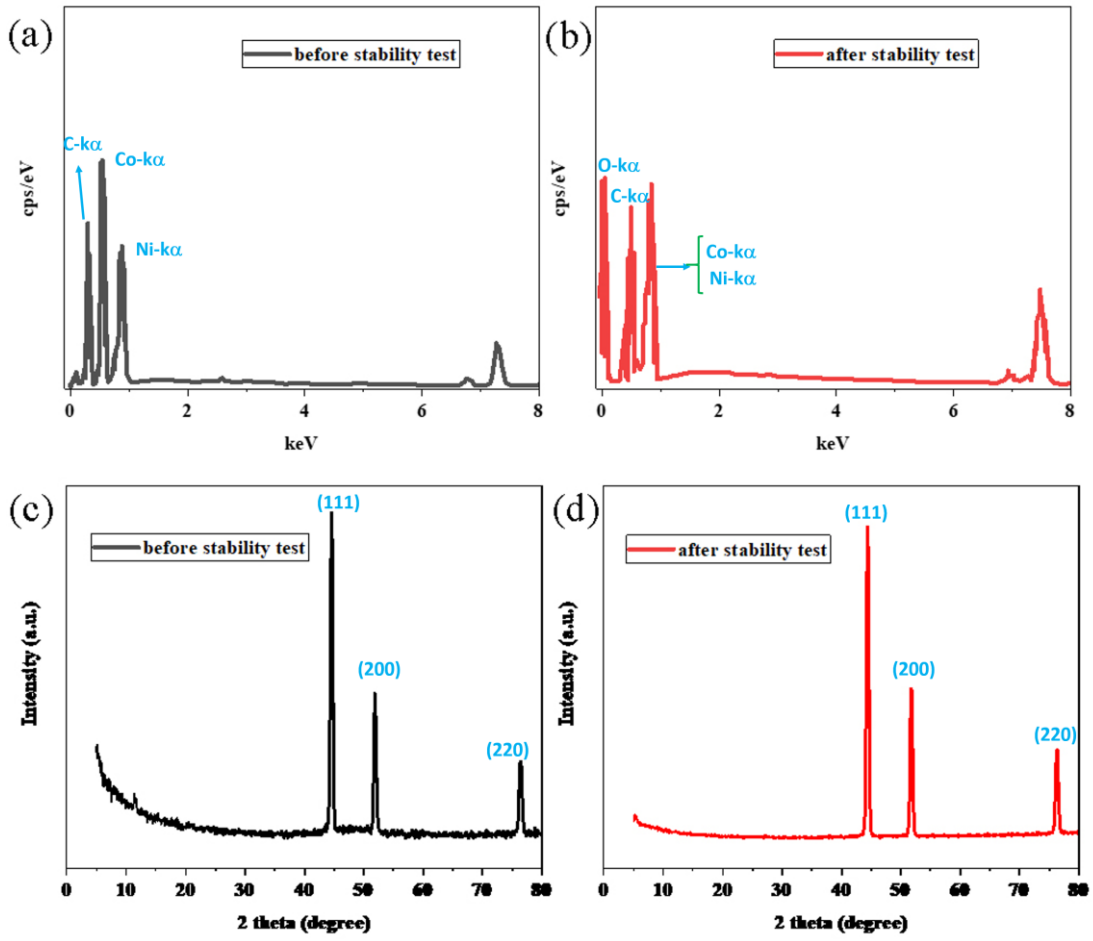

Fig. S7: (a,b) EDS spectrum and (c,d) XRD pattern of $Co_{0.3}Ni_{0.7}$ MOF/3DG before and after stability test. The presence of O-peak is attributed to the oxidation of Co and Ni at 0.7 V (Ag/AgCl).

References

[1] M. Chhowalla, H. S. Shin, G. Eda, L. Li, K. P. Loh, and H. Zhang, "The chemistry of two-dimensional layered transition metal dichalcogenide nanosheets," *Nat. Publ. Gr.*, vol. 5, no. 4, pp. 263–275, 2013.

[2] A. Hatamie, R. Rahmati, E. Rezvani, S. Angizi, and A. Simchi, "Yttrium Hexacyanoferrate Microflowers on Freestanding Three-Dimensional Graphene Substrates for Ascorbic Acid Detection," *ACS Appl. Nano Mater.*, vol. 2, pp. 2212–2221, 2019.

[3] E. Rezvani *et al.*, "Synthesis, First-Principle Simulation, and Application of Three-Dimensional Ceria Nanoparticles/Graphene Nanocomposite for Non-Enzymatic Hydrogen Peroxide Detection," *J. Electrochem. Soc.*, vol. 166, no. 5, pp. H3167–H3174, 2019.

[4] L. Zhao, Shenlong Wang, Yun Dong, Juncai He, Chun-Ting Yin, Huajie An, Pengfei Zhao, Kun Zhang, Xiaofei Gao, Chao Zhang, "Ultrathin metal–organic framework nanosheets for electrocatalytic oxygen evolution," *Nat. Energy*, vol. 1, no. 12, p. 16184, 2016.

[5] Y. Chen, N. Wang, W. Hu, and S. Komarneni, "In situ construction of porous Ni/Co-MOF@ Carbon cloth electrode with honeycomb-like structure for high-performance energy storage," *J. Porous Mater.*, vol. 26, no. 3, pp. 921–929, 2019.

[6] M. Hasanzadeh, A. Simchi, and H. S. Far, "Nanoporous composites of activated carbon-metal organic frameworks for organic dye adsorption: Synthesis, adsorption mechanism and kinetics studies," *J. Ind. Eng. Chem.*, vol. 81, pp. 405–414, 2020.

[7] B. BARDAKÇI, "FTIR-ATR spectroscopic characterization of monochlorophenols

and effects of symmetry on vibrational frequencies," *Cankaya Univ. J. Arts Sci.*, vol. 1, no. 7, pp. 13–19, 2007.

[8] X. Liang, B. Zheng, L. Chen, J. Zhang, Z. Zhuang, and B. Chen, "MOF-derived formation of ni2p–cop bimetallic phosphides with strong interfacial effect toward electrocatalytic water splitting," *ACS Appl. Mater. Interfaces*, vol. 9, no. 27, pp. 23222–23229, 2017.

[9] B. Y. Xia, Y. Yan, N. Li, H. Bin Wu, X. W. D. Lou, and X. Wang, "A metal–organic framework-derived bifunctional oxygen electrocatalyst," *Nat. Energy*, vol. 1, no. 1, p. 15006, 2016.

[10] Y. Han, J. Zhai, L. Zhang, and S. Dong, "Direct carbonization of cobalt-doped NH 2-MIL-53 (Fe) for electrocatalysis of oxygen evolution reaction," *Nanoscale*, vol. 8, no. 2, pp. 1033–1039, 2016.

[11] X. Li, Z. Niu, J. Jiang, and L. Ai, "Cobalt nanoparticles embedded in porous N-rich carbon as an efficient bifunctional electrocatalyst for water splitting," *J. Mater. Chem. A*, vol. 4, no. 9, pp. 3204–3209, 2016.

[12] Q. Dong, Q. Wang, Z. Dai, H. Qiu, and X. Dong, "MOF-derived Zn-doped CoSe2 as an efficient and stable free-standing catalyst for oxygen evolution reaction," *ACS Appl. Mater. Interfaces*, vol. 8, no. 40, pp. 26902–26907, 2016.

[13] X. Zhang *et al.*, "Co/Co9S8@ S, N-doped porous graphene sheets derived from S, N dual organic ligands assembled Co-MOFs as superior electrocatalysts for full water splitting in alkaline media," *Nano Energy*, vol. 30, pp. 93–102, 2016.

[14] M. Ledendecker, S. Krick Calderón, C. Papp, H. Steinrück, M. Antonietti, and M. Shalom, "The Synthesis of Nanostructured Ni5P4 Films and their Use as a Non-Noble

Bifunctional Electrocatalyst for Full Water Splitting," *Angew. Chemie Int. Ed.*, vol. 54, no. 42, pp. 12361–12365, 2015.

[15] M. Luo, Jingshan Im, Jeong-Hyeok Mayer, Matthew T Schreier, Marcel Nazeeruddin, Mohammad Khaja Park, Nam-Gyu Tilley, S David Fan, Hong Jin Grätzel, "Water photolysis at 12.3% efficiency via perovskite photovoltaics and Earth-abundant catalysts," *Science*, vol. 345, no. 6204, pp. 1593–1596, 2014.

[16] S. Liang, Hanfeng Li, Linsen Meng, Fei Dang, Lianna Zhuo, Junqiao Forticaux, Audrey Wang, Zhoucheng Jin, "Porous two-dimensional nanosheets converted from layered double hydroxides and their applications in electrocatalytic water splitting," *Chem. Mater.*, vol. 27, no. 16, pp. 5702–5711, 2015.

[17] D. Liu, Q. Lu, Y. Luo, X. Sun, and A. M. Asiri, "NiCo2S4 nanowires array as an efficient bifunctional electrocatalyst for full water splitting with superior activity," *Nanoscale*, vol. 7, no. 37, pp. 15122–15126, 2015.

[18] X. Wei, N. Li, and N. Liu, "Ultrathin NiFeZn-MOF nanosheets containing few metal oxide nanoparticles grown on nickel foam for ef fi cient oxygen evolution reaction of electrocatalytic water splitting," *Electrochim. Acta*, vol. 318, pp. 957–965, 2019.

[19] S. Chen and S.-Z. Qiao, "Hierarchically porous nitrogen-doped graphene–NiCo2O4 hybrid paper as an advanced electrocatalytic water-splitting material," *ACS Nano*, vol. 7, no. 11, pp. 10190–10196, 2013.

[20] R. Xu, You Tu, Wenguang Zhang, Bowei Yin, Shengming Huang, Yizhong Kraft, Markus Xu, "Nickel Nanoparticles Encapsulated in Few-Layer Nitrogen-Doped Graphene Derived from Metal–Organic Frameworks as Efficient Bifunctional Electrocatalysts for Overall Water Splitting," *Adv. Mater.*, vol. 29, no. 11, p. 1605957, 2017.

[21] M. Zhang, Q. Dai, H. Zheng, M. Chen, and L. Dai, “Novel MOF-Derived Co@N-C Bifunctional Catalysts for Highly Efficient Zn–Air Batteries and Water Splitting,” *Adv. Mater.*, vol. 30, no. 10, p. 1705431, 2018.

[22] X. Liu, J. Dong, B. You, and Y. Sun, “Competent overall water-splitting electrocatalysts derived from ZIF-67 grown on carbon cloth,” *RSC Adv.*, vol. 6, no. 77, pp. 73336–73342, 2016.

[23] J.-S. Xin, Weili Jiang, Wen-Jie Lian, Yajuan Li, Hui Hong, Song Xu, Sailong Yan, Hong Hu, “NiS2 nanodotted carnation-like CoS2 for enhanced electrocatalytic water splitting,” *Chem. Commun.*, vol. 55, no. 26, pp. 3781–3784, 2019.

[24] X. Du, Q. Wang, Y. Li, and X. Zhang, “Oxide/sulfide-based hybrid arrays as robust electrocatalysts for water splitting,” *Dalt. Trans.*, vol. 47, no. 30, pp. 10273–10280, 2018.

[25] L. Jiao, Y. X. Zhou, and H. L. Jiang, “Metal-organic framework-based CoP/reduced graphene oxide: High-performance bifunctional electrocatalyst for overall water splitting,” *Chem. Sci.*, vol. 7, no. 3, pp. 1690–1695, 2016.

[26] J. Lin, Jinghuang Yan, Yaotian Li, Chun Si, Xiaoqing Wang, Haohan Qi, Junlei Cao, Jian Zhong, Zhengxiang Fei, Weidong Feng, “Bifunctional Electrocatalysts Based on Mo-Doped NiCoP Nanosheet Arrays for Overall Water Splitting,” *Nano-Micro Lett.*, vol. 11, no. 1, p. 55, 2019.

[27] M. Jamesh, S. Kumar, and T. S. N. S. Narayanan, “Electrodeposition of hydroxyapatite coating on magnesium for biomedical applications,” *J. Coatings Technol. Res.*, vol. 9, no. 4, pp. 495–502, 2012.